

Sunlight-Duo: Exploiting Sunlight for Simultaneous Energy Harvesting & Communication

Talia Xu

Delft University of Technology
Delft, Netherlands
m.xu-2@tudelft.nl

Patrizio Manganiello

Delft University of Technology
Delft, Netherlands
p.manganiello@tudelft.nl

Mirco Muttillo

Delft University of Technology
Delft, Netherlands
m.muttillo@tudelft.nl

Harald Haas

University of Cambridge
Cambridge, UK
huh21@eng.cam.ac.uk

Miguel Chavez Tapia

Delft University of Technology
Delft, Netherlands
m.a.chaveztapia@tudelft.nl

Marco Zuniga Zamalloa

Delft University of Technology
Delft, Netherlands
m.a.zunigazamalloa@tudelft.nl

Abstract

Sunlight has been used for decades to *harvest energy* and more recently to *transmit wireless data*. We present a novel system that exploits sunlight to achieve both *energy harvesting* and *communication*, enabling in that way a sustainable system that relies *solely* on natural light. Sunlight can be modulated with different optical devices, but demodulating sunlight with solar cells playing the dual role of energy harvesters and data receivers presents a challenge that has not been tackled yet. This challenge exposes a fundamental trade-off between energy harvesting and communication. High sunlight intensity favors energy harvesting but also creates a high source of interference because sunlight provides both, the signal (S) and noise (N). Thus, *an open research question is whether solar cells can operate as harvesters and receivers with sunlight*. To answer this question, we perform a thorough analysis of various solar cell configurations suitable for embedded IoT devices. Our analysis reveals that sunlight can be used for simultaneous energy harvesting and data reception, but the receiver must adjust key solar cell parameters on the fly. Based on our analysis, we build a *self-powered* prototype and test it in different conditions. Our prototype maintains a bi-directional link for up to 11 m, with a data rate of 1200 bps for downlink and 800 bps for uplink. Additionally, our system maintains a stable link over 2 m throughout the daytime. To the best of our knowledge, this is the first work using sunlight simultaneously for energy harvesting and communication.

CCS Concepts

- Networks → Physical links;
- Hardware → Emerging technologies;

Keywords

Wireless Communication, Simultaneous Energy Harvesting and Communication

1 Introduction

Since its invention in the 19th century, wireless communication has predominantly relied on the RF spectrum. However, during the last decade, there has been an unprecedented demand on this spectrum [7]. In response to this challenge, researchers have started exploring visible light communication (VLC). By modulating the intensity of an LED at a high speed, wireless transmissions can be

achieved without disturbing illumination, offering a yet unexploited spectrum [13, 21]. *In indoor scenarios*, VLC is practical because there is not much interference from sunlight and a small energy overhead is needed to add communication over illumination. *In outdoor scenarios*, VLC is less effective due to the strong presence of ambient light. Receivers based on *photodiodes* tackle interference through the use of elaborate optical enclosures and automatic gain control mechanisms. To mitigate the shortcomings of photodiodes, researchers have demonstrated the potential of solar cells to serve the dual purpose of energy harvesters and data receivers [8, 9, 22]. Given that solar cells are designed, from inception, to handle high illumination, it is advantageous to re-purpose them as receivers. However, *the fundamental limitation of the SoA is that solar cells are used as receivers but only with transmitters using high-power lights* [22] or *carefully selected lasers* [8, 9]. Using artificial light sources for transmission misses the opportunity to leverage the pervasive presence of sunlight as a wireless carrier.

An alternative approach in leveraging the omnipresence of sunlight for communication is termed *passive-VLC*. Unlike VLC, passive-VLC does not need to modulate an artificial light directly [26]. Instead, it modulates ambient light using optical surfaces, such as liquid crystal shutters (LCs). *The limitation of passive-VLC systems is that the receivers still use photodiodes, which miss the opportunity for energy harvesting and necessitate the use of elaborate optical designs to limit sunlight interference*.

Motivation. We envision a new communication paradigm for embedded IoT devices to harness sunlight for communication and energy harvesting. This paradigm merges the most sustainable features of passive-VLC (using sunlight to transmit data) and outdoor-VLC (employing solar cells to harvest energy and receive data).

Our prototype introduces a novel use of sunlight collectors, as illustrated in Figure 1. Sunlight collectors capture natural light and redirect it to *indoor* spaces, but we show that these collectors can also be exploited outdoors¹. The beams radiated by the sunlight collector are modulated using liquid crystals, and the receiver is a battery-less device that uses solar cells to obtain energy and data from the sunlight beams. The receiver also has a reflective surface to communicate back to the transmitter, creating a bi-directional link. A potential application of our system is within the realm of

¹A sunlight collector consists of a lens system and a motor to follow the sun's position. While it's feasible to develop a compact, custom-made sunlight collector, we chose a commercial variant to reduce the design time.

smart farming, where a central unit (sunlight collector) could issue commands to retrieve data from nearby sensors.

Our system is not envisaged to replace low-power RF, but rather to provide a new perspective. A key advantage of light communication is the access to an open and unrestricted spectrum; and considering the increasing use of solar cells in small IoT devices, these cells could be dubbed as receivers.

Key challenge. Exploiting sunlight for communication and energy harvesting exposes a challenge that has not been investigated before: *We need to optimize solar cells not only as harvesters but also to decode a signal that is embedded in sunlight.* Sunlight provides the signal (S) but also noise (N). In outdoor-VLC, sunlight interference is reduced by using artificial sources, such as lasers [8, 9], that transmit data within the weakest portions of the sunlight spectrum. With such configurations, the spectra and intensity of the transmitter (laser) are carefully designed to differ as much as possible from sunlight. In passive-VLC, sunlight interference is limited by creating optical enclosures around photodiodes; and the only task is communication, there is no harvesting. In our scenario, the signal and noise share the same spectrum and similar intensity, affecting the operation of solar cells to perform both as receivers and harvesters.

Contributions. Considering the above motivation and challenges, our work makes the following contributions.

Contribution 1 [section 4]: Analysis of solar cell chargers and configurations. To gain a deep understanding of the charging and communication behavior of solar cells, we carry out a thorough analysis considering different ambient light intensities and solar cell configurations. This analysis provides key insights for designing a front end that can meet different charging and communication needs.

Contribution 2 [section 5]: Dynamic reconfiguration scheme. After identifying the configurations that perform best, we evaluate the performance of our passive link over a complete *charging cycle*. Based on the insights, we design a dynamic reconfigurable scheme that maintains a high level of energy harvesting while optimizing for communication.

Contribution 3 [section 6]: Prototype and evaluation. Using sunlight for simultaneous energy harvesting and communication, our prototype achieves more than 90% packet success rate at a distance of 11 m for both uplink and downlink, with a data rate of 1200 bps and 800 bps, respectively. Our results also show that we can establish a stable link from 9 am to 7 pm. During this time, our receiver

harvests enough power to support the decoding process and three extra sensors and an e-ink display. This is the first demonstration of a link relying solely on sunlight for communication and power.

Historical context. In 1880, Alexander G. Bell built the first sunlight link. The transmitter was a megaphone connected to a reflective surface to modulate voice using sunlight, and the receiver was a rudimentary photosensor. Bell called his invention the Photophone and in a letter to his father wrote “*I have heard articulate speech by sunlight! I have heard a ray of sun laugh and cough and sing!*”. Sunlight-Duo (Sunlight-Duo) is a stepping stone towards converting the Photophone into an eco-friendly link using sunlight for transmission and solar cells for reception and energy.

2 System overview

Similar to most passive-VLC studies, our system has three components: the *light source*, the *transmitter*, and the *receiver*. *Our main contribution is on the receiver.* In this section, we describe these components and the challenge of designing a solar cell receiver.

Light Source: Various elements can emit ambient light, functioning as a *source*, *interference*, or both, as shown in Figure 2a. The source’s light is modulated by an optical surface (transmitter). In most passive-VLC studies, the source and interference are distinct. For example, in [25, 29], a flashlight is used as the source and other light bulbs act as interference. This setup provides stable links because the source light is much stronger and more focused than the ambient light, and they have different spectra. In other studies, the source and interference come from the same point, typically the sun [6, 11]. This setup is more complex because the source and interference have the same spectrum, completely mixing the signal and noise. Furthermore, the sun intensity changes throughout the day. This more challenging setup is the one tackled in our work, with the added complexity of using solar cells as receivers, instead of photodiodes.

Transmitter: The transmitter is an optical device that modulates ambient light by changing some of its properties. Two types of optical surfaces have been studied as transmitters, liquid crystals (LCs) [16, 25, 29, 31] and Digital-Micromirror-Devices (DMDs) [30]. DMDs achieve a higher data rate but require a complex driver. Since most studies rely on LCs, we build upon the SoA designs using LCs due to their simpler modulation.

An LC has two states, which either block or allow light to pass through depending on the voltage applied to its pins. LCs are simple to drive but have slow rise/fall times. Most systems employing LCs and photodiodes have demonstrated data rates between 100 bps and 8 kbps [6, 11, 16, 25, 29, 31]. Since our focus is on the receiver, we build upon the SoA designs consisting of *single* LCs [6, 16, 31]. Our platform uses a PI-cell LC with a switching speed around 600 Hz, c.f. Figure 2e (1.34 ms and 0.15 ms for the rise and fall times). This speed is sufficient to attain full contrast. Since we use frequency-shift keying modulation, we can attain faster switching speeds, at the cost of lowering the contrast, as described in section 5.

Our work uses two setups to analyze interference: controlled and in-the-wild. The *controlled* setup is used in section 4, where we rely on artificial lights to emulate an outdoor lighting scenario. This controlled setup allows a systematic assessment of solar cell performance in terms of their charging and communication behaviors. Figure 2d depicts the transmitter used in this setup, where the

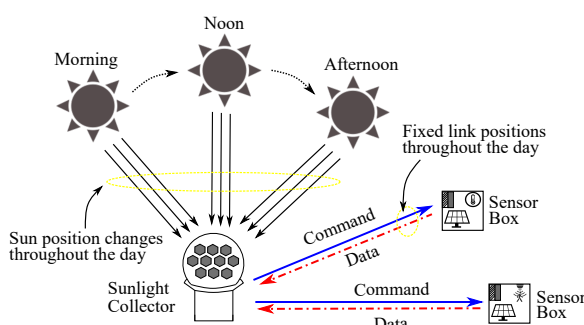


Figure 1: An overview of our approach.

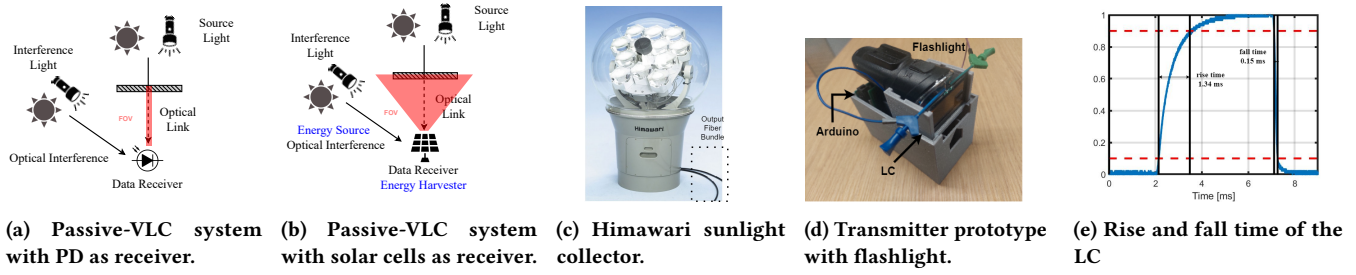


Figure 2: System overview and components.

beam emitted by a flashlight is modulated via an LC controlled with an Arduino. The *on-the-wild* setup is used in our final evaluation (section 6). In that setup, the sun provides the interference and the flashlight is replaced with the output of the sunlight collector to radiate a natural light beam towards the LC. The output of the sunlight collector has bundles of optical fibers to direct the light from the tracking lenses to the desired direction (Figure 2c). This final evaluation exclusively uses sunlight for both energy harvesting and communication.

Receiver: Prior passive-VLC studies leveraging sunlight for communication employ photodiodes. However, photodiodes require substantial power and a complex optical design to prevent saturation outdoors [6, 11]. Moreover, in strong sunlight conditions, outdoor-VLC studies indicate that solar cells outperform photodiodes as receivers [19]. Contrary to the power-consuming nature of photodiodes [15], solar cells generate power while receiving information, but they introduce a challenge in the design, as demonstrated in Figure 2b. Unlike photodiodes, which allow for reducing the field-of-view (FoV) to eliminate interference, solar cells inherently have a broad FoV that cannot be reduced without significantly hampering their energy-harvesting potential.

Overall, our work targets a scenario that has not been considered before, one where *sunlight is the common source of three components: energy, data, and interference*. Therefore, it is important to analyze different levels of ambient light and solar cell configurations to achieve joint energy harvesting and communication.

3 State-of-the-Art analysis

In this section, first, we position our work within the general areas of ambient backscattering and positive energy sensing, and after that, we discuss in detail the areas of outdoor- and passive-VLC.

3.1 Passive RF & positive-energy sensing

Ambient RF energy harvesting for battery-less transmissions has gained traction. That approach exploits ubiquitous RF signals (e.g., TV, WiFi, BLE, LoRa) to create passive wireless links [5, 18, 24]. RF backscattering relies on energy-intensive man-made signals, unlike natural light, which uses an energy-free wireless carrier.

Positive-energy sensing involves sensors harvesting energy for their own operation and additional tasks. Some studies use photodiodes (PDs) [17] while others use solar panels [20] for energy harvesting and close-proximity hand gesture recognition. These techniques require gestures to be made a few centimeters away and capture under 10 samples per second. While these approaches utilize ambient light, they don't fully exploit solar cells' sensing capabilities in speed and range.

3.2 Solar Cell as a Data Receiver

A taxonomy highlighting the novelty of our work w.r.t. the most relevant studies in the SoA is presented in Table 1 and a quantitative comparison in Table 2.

Table 1: Relevant Communication Systems in the SoA

Signal Source \ Energy Source	Sunlight	Artificial Light	External Power ¹
Sunlight	 This work		 Passive VLC
Artificial Light (LED, Laser)	 Outdoor VLC	 Indoor VLC	 Solar Cell as Data Receiver

¹ External power required, not provided by the receiver (PD or solar cell)

Solar Cells as Data Receivers: cell (5) in Table 1. As solar cells have been traditionally used as energy harvesters, early research efforts aimed at demonstrating the potential of solar cells to work as data receivers. For instance, Wang et al. showcased impressive communication speeds of 7.01 Mbps and 11.84 Mbps over 39 cm using an LED transmitter and a 4.5 W solar cell receiver [27, 28]. Moreover, Lorrière et al. showed that solar cells could outperform PDs under intense sunlight [19]. These studies, however, use solar cells *solely* as receivers, requiring external batteries to operate, and neglect their inherent energy harvesting potential. Other studies explore workarounds such as alternating between charging and sensing, yet this method reduces efficiency and requires careful synchronization between the transmitter and receiver [10, 23].

Simultaneous charging and communication, but using only artificial light as an energy and signal source: (4) in Table 1. Mir et al. conducted a study where an LED transmitted information to a solar cell receiver that could simultaneously harvest energy and decode data [22]. The study analyzes the impact of various solar cell configurations. Their findings indicate that a parallel configuration of solar cells performs more effectively for charging, while a series configuration excels in communication. While these insights are

valuable, they are derived from an *indoor scenario using light bulb and without interference*. In our work, we show that these findings are not applicable in outdoor scenarios as the performance of both, charging and communication, degrades significantly outdoors.

Simultaneous charging and communication, but using sunlight as an energy source and artificial light as a signal source: (3) in Table 1. A few outdoor-VLC studies demonstrate the potential for simultaneous communication and energy harvesting using solar cells. However, these studies rely on *artificial* light sources for the signal. Das et al. created an outdoor link with a 940 nm laser. This wavelength is chosen because sunlight is highly attenuated by the atmosphere in that portion of the spectrum. In this way, the communication link performance is guaranteed due to minimal interference. Contrary to this approach, we propose a system where sunlight is used for data transmission, eliminating the requirement for a separate artificial source for communication.

3.3 Sunlight as a Signal Source

This section describes the relevant work on passive-VLC systems, (2) in Table 1. These systems capitalize sunlight solely as a signal source, but not as an energy source. Luxlink [6] and Chromalux [11] leverage the intense illumination from sunlight to enable long-range communication without the need for artificial sources. Luxlink achieved a range of 65 m using sunlight, although with a limited data rate of 80 bps. Chromalux, meanwhile, covered a distance of 50 m achieving a data rate of 1 kbps. Despite these achievements, both studies opt for photodiodes (PDs), which do not harvest energy and perform sub-optimally as outdoor receivers compared to solar cells [19].

3.4 The novelty of our approach

Overall, our work advances the SoA in two main ways, cell (1) in Table 1. Compared to studies requiring external power –using either PDs, as in (2), or solar cells solely as sensors, as in (5)– our platform is self-powered by the receiver. And compared to studies using solar cells for simultaneous energy harvesting and decoding –either indoors (4) or outdoors (3)– our transmitter does not require any artificial source. A detailed comparison with SoA studies is presented in Table 2. Sunlight-Duo is the only system using sunlight for power and communication. The most relevant works are the ones working outdoors (bottom six rows), where the green and orange colors capture their main pros and cons². In the next section, we analyze how a low-power IoT device can optimize harvesting and reception using a small solar cell array.

4 Analysis of Charger and Solar Cell

Using the same solar cells for communication and energy harvesting, while relying solely on sunlight for both tasks, presents a complex scenario. Specifically, there are two main challenges, (*i*) the divergent optimal conditions for charging and communication; and (*ii*) the complexity of decoding the signal embedded under the high intensity of sunlight. To tackle these challenges, we first perform an in-depth analysis of solar cell characteristics in a *controlled* scenario, focusing on two main components:

²A general trade-off between passive- and active-VLC (last column) is to reduce power consumption (by using ambient light) at the cost of reducing the data rate (due to the slow optical surfaces) [6, 11, 16, 25, 29, 31]

- (1) The type of charger, which runs the algorithm designed to optimize the energy harvesting of the solar cells.
- (2) The configuration of inter-cell connections, as this plays a pivotal role in optimizing the balance between harvesting and communication functionalities.

4.1 Controlled evaluation setup and metrics

To design our system for varying sunlight conditions, we need to understand solar cell behavior under dynamic lighting. We conduct controlled experiments using two light fixtures for separate energy harvesting and communication purposes, allowing us to regulate harvesting, signal, and noise intensities independently. A 100 W LED array simulates sunlight *interference*, and a white light *source* behind an LC shutter acts as the data transmitter, with the *source's* spectrum falling within the *interference's* range to emulate data transmission via sunlight.

A diagram of the experimental setup is shown in Figure 3. The output of the solar cell goes through a high-pass filter (top branch, used for communication) and a low-pass filter (bottom branch, used for charging). Our design follows a battery-less approach, using a supercapacitor as energy storage, instead of a battery, due to the detrimental effects that batteries have on the environment. V_s represents the sensing voltage used to decode data, and V_{batt} represents the supercapacitor voltage. The signals received by both branches are shown in the bottom-right plot. We can observe a DC component used for energy harvesting (flat red line) and an AC component (yellow curve) containing the data.

Metrics. The *charging performance* is measured by the time it takes to charge the supercapacitor. The *communication performance* is measured by calculating the received signal strength (RSS) using a triangular wave within a time window of 10 ms.

Generalization. As described later, our dynamic reconfiguration requires some parameters to optimize harvesting and communication. These parameters depend on the type of solar cell and charger used. Since it is not possible to evaluate all possible combinations of solar cells and chargers, to generalize our method, we provide a step-by-step framework. The parts presented inside boxes are given as general guidelines to implement our approach.

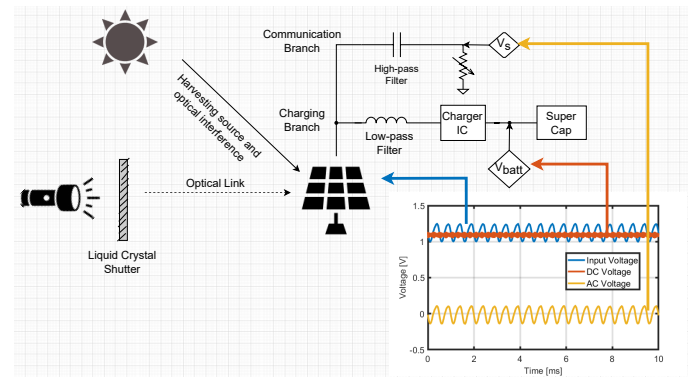


Figure 3: Controlled setup with solar cells.

Table 2: Comparison of Sunlight-Duo with the most relevant systems in SoA.

Name	Signal	Power	Signal Strength	Sunlight Interference	Speed	Range	Solar Cell Model	Location	Sim. S/C	System
[27]	LED	External	3.5W/m ²	Yes (<10% signal)	7.01 Mbps	39 cm	SX305M (4.5W)	Indoor	No	active
[28]	LED	External	7W/m ²	No	11.84 Mbps	N/S ¹	SX305M	Indoor	No	active
[22] ²	LED	LED	N/S	No	N/S	N/S	Variable	Indoor	Yes	active
[19]	LED	External	5080 lux	Yes (400W/m ²)	1.2 MHz	23 cm	Solar Frontier PV Module	Outdoor	No	active
[8]	Laser	Sunlight	8.7W/m ²	Yes	8 Mbps	30 m	5 W Silicon Solar Cell	Outdoor	Yes	active
[9]	Laser	Sunlight	N/S	Yes	6.34 Mbps	3.5 m	5 W Silicon Solar Cell	Outdoor	Yes	active
[6]	Sunlight	External	Variable	Yes	80 bps	50+ m	N/A ³	Outdoor	No	passive
[11]	Sunlight	External	Variable	Yes	1.2 kbps	50+ m	N/A ³	Outdoor	No	passive
Sunlight-Duo	Sunlight	Sunlight	Variable	Yes	1.2 kpbs	11 m	KXOB25-14X1F	Outdoor	Yes	passive

¹ N/S stands for 'not specified'.² This studies implements a LiFi downlink and an RF uplink.³ Photodiodes were used in place of solar cells.

4.2 Step 1: Choosing a solar cell charger

Solar cells need to be connected to a charger IC to manage the energy harvesting process. Given that IoT sensors have limited surface areas. The first step is to select a charger IC that ensures maximum charging efficiency within the spatial constraints and under different amounts of ambient light.

Charger ICs run algorithms that consume part of the power harvested by the cells. With large solar panels, the power consumed by the charger is a tiny fraction of the power generated by the solar cells [4]. Since IoT devices operate on a significantly smaller scale, the energy consumption of some algorithms can offset their benefits. Our design adopts a solar cell area of 3000 mm², which is commonly used in this area [22]. In this first step, the focus is solely on the harvesting aspect of the system. Therefore, only the LED sunlight emulator in Figure 3 is utilized.

Among maximum power point tracking (MPPT) algorithms, the Perturb and Observe (P&O) and Constant Voltage (CV) methods are the most prevalent. To better understand which algorithm is better suited for small IoT devices, we evaluate one solar cell charger with a P&O algorithm (the SPV1040) and one with a CV (the BQ25570). The results in Figure 4 reveal that the CV algorithm (red curves) consistently outperforms the P&O (blue curves) across all light conditions. With small solar cells, the power consumed by the more accurate algorithm (P&O) outweighs the gains obtained from it. Furthermore, under low light intensities (10 klux and 3 klux), P&O even fails to store enough power to run itself, failing to charge the supercapacitor beyond 1 V.

After this step, the design will be guaranteed to have the best charger. In our case, we utilize the BQ25570 charger due to the superior performance of the CV algorithm.

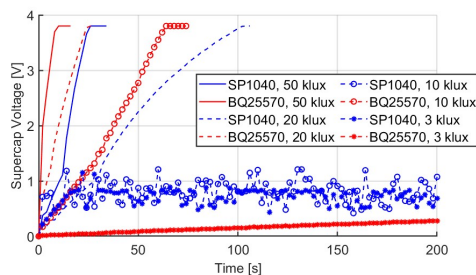


Figure 4: Charging a 22mF supercapacitor with different charger ICs under different light intensities.

Table 3: Solar Cell Reconfigurable Parameters

Parameter	Configuration
Solar Cell Connection	2s-8p, 4s-4p, 8s-2p
Operating point η_{voc}	80%, 50%, 30%, 10%

4.3 Step 2: Defining Solar Cell Configurations

After selecting the best charger, the next step is to define the different solar cell *configurations*. Denoting n as the number of cells that can be placed on the device's surface, we need to analyze the best configuration for those n cells, from serial to parallel. These configurations play a central role in defining the performance of energy harvesting and reception.

We populate the available area (3000 mm²) with 16 Anysolar KXOB25-14X1F solar cells. With an efficiency of 25%, these cells capture the most popular technology in the market. For n solar cells, the *connection* refers to the number of cells connected in series and in parallel. To analyze, the trade-off between communication and charging, we explore three configurations: 8 parallel sets of 2 solar cells in series (2s-8p), 4 parallel sets of 4 solar cells in series (4s-4p), and 2 parallel sets of 8 solar cells in series (8s-2p).

For a given area and number of solar cells, the configurations cannot be arbitrary, they need to satisfy two key criteria: 1. Equal current and voltage flow in each branch, maximizing the solar cell's efficiency, and 2. Ensuring the maximum current and voltage are within a valid range for chargers designed for low-power applications.

With our different configurations, we evaluate the harvesting and communication capabilities under varying light intensities. To benchmark the signal strength, the flashlight is turned on behind the LC, while the LC is modulated to transmit a triangular wave at a fixed frequency of 2 kHz. The power of the emulated sunlight ranges from 3k lux to 50k lux, which is typical during daylight. In our analysis, we consider two configuration parameters: the connection structure (whether it is more in series or parallel) and the operating point (represented by η_{voc} and described later in detail).

After this step, the design has a charger, two or more configurations depending on the number of cells, and different operating points η_{voc} . A summary of these parameters for our case is shown in Table 3. Next, we explain the values chosen for each parameter and evaluate their impact under the different operational stages of the charger.

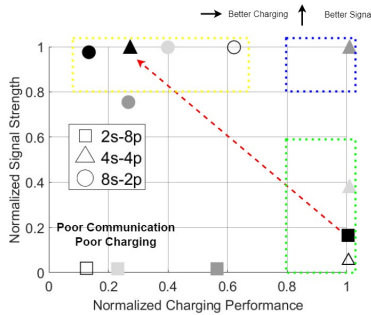


Figure 5: Communication and charging in the precharging stage. Colors denote varying light intensities: black - 3 klux; dark grey - 10 klux; light grey - 20 klux; and white - 50 klux.

4.4 Step 3: Analyzing the Pre-charging Stage

When the system begins operating from a cold start, the supercap does not have sufficient energy to run the MPPT algorithm in the charger IC. The charger can harvest energy but in a suboptimal manner. Thus, in the pre-charging stage, the main requirement is to identify the solar cell *connection* that can charge the supercap as fast as possible.

To analyze this stage, we consider four ambient light intensities depicted with different colors in Figure 5: white 50 klux, light grey 20 klux, dark grey 10 klux, and black 3 klux. To leave the pre-charging stage, the supercap's voltage needs to go above the operational threshold of 1.8 V. Each connection is represented by a different shape: a square for the more *parallel* connection (2s-8p), a triangle for the *mixed* connection (4s-4p), and a circle for the more *serial* connection (8s-2p). The metrics are *normalized for each lighting condition*. The closer to the right a symbol is, the faster the charging; and the closer to the top, the better the communication.

Ideally, we want a single configuration (triangle, circle or rectangle) to deliver the best performance for all lighting conditions (all colors in the top right corner, blue region). This would indicate that a single configuration could simultaneously optimize charging and communication regardless of the intensity of sunlight. However, Figure 5 shows that this is not the case. There is only one light condition, 10 klux, where there exists an optimal configuration for charging and communication, the *mixed* (triangle) setup 4s-4p.

In Figure 5, we identify two key regions: one (yellow rectangle) with configurations favoring communication over charging, and another (green rectangle) with the opposite trade-off. This Pareto frontier suggests that the receiver would need to switch configurations that can only optimize one task. For example, under low light (3 klux, black markers), favoring communication over charging (red arrow) would increase the charging time fourfold, from a normalized performance of 1 (*parallel* setup, black square) to 0.25 (*mixed* setup, black triangle).

Overall, considering that in the pre-charging stage, the MPPT algorithm is not running optimally, it is better to use a connection that prioritizes charging over communication whenever possible.

4.5 Step 4: Analyzing the Charging Stage

In the pre-charging stage, the analysis of solar cells includes only the connection (serial, mixed, parallel) because the harvesting algorithm could not run the operating point η_{Voc} . In the charging stage, the algorithm is operational. Thus, we need a deep analysis of the critical influence of the operating point in tandem with the solar cell's connection.

The charging stage begins once the supercap's voltage exceeds 1.8 V. At this point, the MPPT algorithm is fully active. The receiver spends most of its operational time in this stage, hence, it is critical to optimize harvesting and communication. To achieve this optimization it is necessary a clear understanding of the MPPT algorithm and its parameter η_{Voc} . Next, we explain how the CV algorithm changes the operating point η_{Voc} , and then, present the results of our analysis under different configurations and lighting conditions.

Algorithm operation and operating point η_{Voc} . The Constant Voltage (CV) algorithm starts by disconnecting the load to measure the *open circuit voltage* (V_{oc}). The system then regulates the charging process by maintaining the output voltage at a constant percentage of V_{oc} , represented by the variable η_{Voc} . On the BQ25570, the algorithm temporarily halts the harvesting process every 16 s to sample the V_{oc} and then sets $\eta_{Voc} = 80\%$. While this percentage may be optimal for power output, lower values of η_{Voc} could be better for communication. In this section, we assess the impact of deviating from the optimal charging point to improve communication. The notation used to describe a given connection and operating point is $X_s - Y_p - \eta_{Voc}$. For instance, a configuration labeled as 4s-4p-50 denotes a solar cell operating with a *mixed* connection at $\eta_{Voc} = 50\%$.

Charging and communication efficiency. The results of our analysis are presented in Figure 6. The performance of individual operating points (10%, 30%, 50%, 80%) is illustrated from Figure 6a to Figure 6d, while Figure 6e displays the combined Pareto frontier. Overall, our analysis provides three main results.

First, the range of the operating point η_{Voc} should be between 10% and 80%. For $\eta_{Voc} = 80\%$ (Figure 6d), several configurations provide almost optimal charging (close to 100%) but low communication performances (mainly below 40%). As we reduce the value of η_{Voc} (Figure 6c), the charging performance decreases (remaining below 70%) but the communication improves. For $\eta_{Voc} = 30\%$ and $\eta_{Voc} = 10\%$, the trend continues, with communication giving a better performance than charging.

Second, similar to the pre-charging stage, there is no configuration (same connection and operating point) optimizing charging and communication simultaneously for all light intensities. At $\eta_{Voc} = 30\%$, the best connections are parallel and serial; while at $\eta_{Voc} = 50\%$ and $\eta_{Voc} = 80\%$, the best connections are mixed and parallel. This variability occurs because there is a delicate balance between the type of connection, the value of the operating point, and the light intensity. The currents generated for charging and sensing need to be optimized for both tasks, while avoiding saturation, in particular at high-intensity levels.

Third, our analysis allows defining a **Pareto frontier** where one connection (serial, circles) plays the most critical role. In Figure 6e, we show the best Pareto frontier after combining all connections

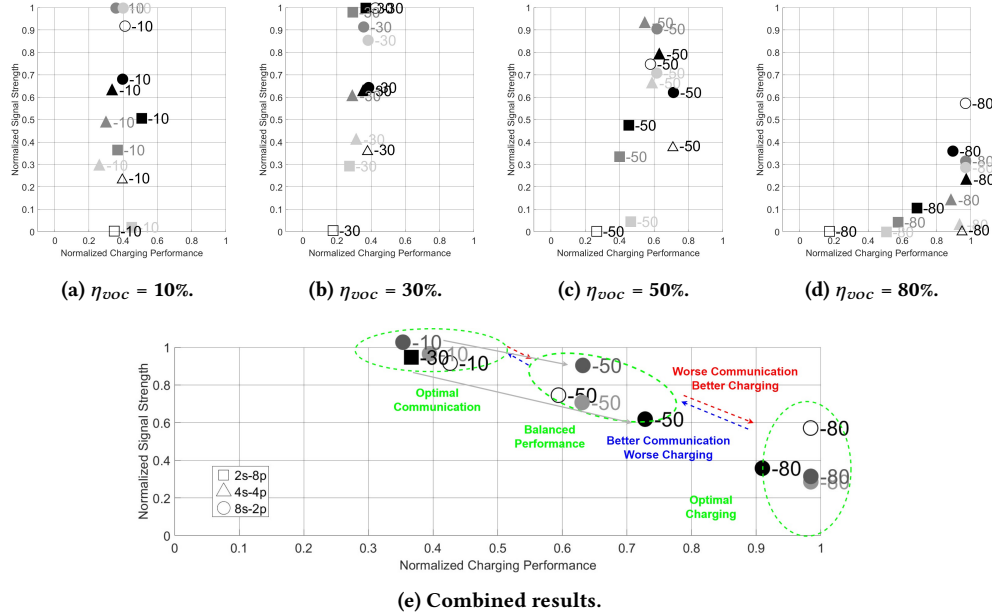


Figure 6: Communication and charging characteristics of the solar cell receiver during the *charging* stage. Colors denote varying light intensities: black - 3 klux; dark grey - 10 klux; light grey - 20 klux; and white - 50 klux.

and operating points. While building a Pareto frontier, it is important to make sure that the entire boundary is populated with configurations that include all light intensities (color). In our Pareto frontier we can observe that, except for one marker, the boundary is covered completely by the serial connection (circles) with operating points ranging from 10% to 80%. Adjusting the operating point can prioritize communication ($\eta_{voc} = 10\%$), charging ($\eta_{voc} = 80\%$), or maintain a balance ($\eta_{voc} = 50\%$). Our Pareto frontier can maintain an effective trade-off without requiring a significant compromise.

The only exception for the serial configuration is when the receiver needs to optimize communication (top green ellipse) under low light conditions (3 klux). This exception is 2s-8p-30 (black square), a parallel setup with $\eta_{voc} = 30\%$. This exception, however, is not critical. At low light intensities, charging may be more relevant, and hence, the receiver could use the serial configuration with $\eta_{voc} = 50\%$ to double the charging efficiency, from 36% to 72%, at the cost of reducing the communication efficiency from 95% to 60%, as depicted by the gray arrow between the black square and black circle.

Based on the charging stage analysis, our final design uses the serial connection with four operating points. Other combinations of chargers and solar cells may lead to different configurations. The analysis of connections and operating points is detailed but only needs to be done once.

4.6 Step 5: Operation in Fully-charged Stage

When the supercapacitor is fully charged, the charger ensures that no further power flows into the supercapacitor to avoid overcharging it. As a result, communication cannot be carried out effectively because the system operates near the open circuit voltage. To enable communication we disconnect the supercapacitor and connect the DC branch to a fixed load to allow a flow of current in the high-frequency branch. When the supercapacitor voltage drops below a certain point, the supercapacitor is reconnected.

4.7 Summary

Our analysis shows that it is possible to achieve energy harvesting and communication with natural light. In the precharging phase, the system focuses on charging instead of communication. This design choice is not a limiting factor because, for battery-less systems deployed outdoors, the precharging phase only takes a few seconds at the beginning of each day. It is only during that short period of time that communication is affected. During the charging phase, which is the most prevalent, the ability to reconfigure the operating points allows attaining a wide range of trade-offs, from near-optimal charging to near-optimal communication without penalizing either completely. During the fully-charged phase, the system can solely focus on optimizing communication. As shown later in our evaluation, these insights cover a design space that has not been tackled yet.

5 Design of Reconfigurable Receiver

In the previous sections, the receiver configuration was analyzed for various controlled scenarios. In this section, we design a scheme to automatically adapt the receiver's configuration in real time depending on the ambient light intensity.

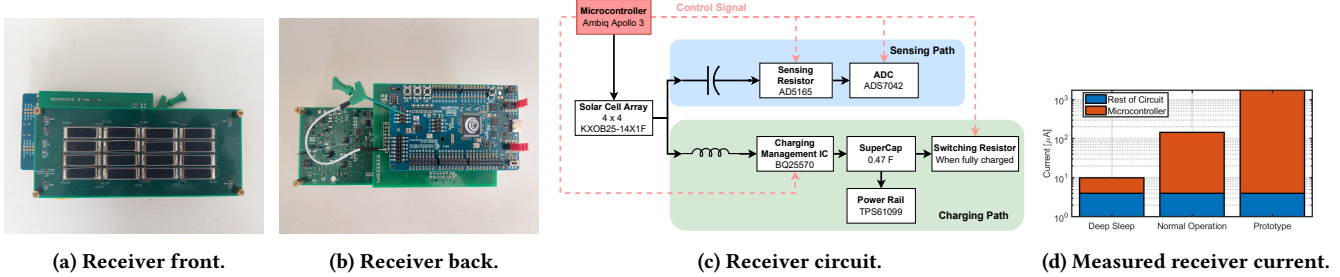


Figure 7: Receiver design and power consumption

5.1 Receiver Hardware

The prototype and the circuit diagram are illustrated in Figure 7a, Figure 7b, and Figure 7c. The design employs low-power components, facilitating batteryless operation in outdoor conditions. In our prototype, the most power-intensive component is the microcontroller. We use the Ambiq Apollo 3 evaluation board, which features non-removable and non-disabling modules, thereby consuming a total of 2 mA [1]. However, the Ambiq Apollo3 microcontroller is documented to consume 140 μ A under normal operation and 6 μ A in deep sleep mode. Thus, with a custom design, the current power consumption of our prototype could be further reduced. The rest of the circuit draws 4 μ A.

Modulation: The experiment setup is similar to section 4. But instead of sending a triangle wave, the transmitter continuously sends "Hello World" at 400 bps. We use binary frequency shift keying (BFSK) for signal modulation. Despite its lower data rate, FSK's inherent noise resistance proves beneficial for outdoor environments with dynamic light intensities [6]. We use a 1600 Hz signal to represent a '0' and a 2000 Hz signal to represent a '1'. We adopt a data link layer where the packet starts with an SYN symbol (01010101). The ASCII payload is preceded by an STX (Start of Text, 00000010), followed by ETX (End of Text, 00000011) and ETB (End of Transmission Block, 00010111).

Demodulation: The decoding is done as follows:

Preamble detection: A sliding window equivalent to one bit is applied to the received signal. Within this window, an FFT is applied to identify the frequency component with the largest magnitude.

Data demodulation: After a SYN byte is identified, the remaining bytes are decoded with the same process. If an ETX is identified, the received packet is recorded.

Phase correction: During preamble detection, if the decoded bit is different from the previous bit, the receiver adjusts the sliding window to synchronize to the phase of the transmitter.

FFT optimization: The CMSIS library on the Ambiq Apollo 3 facilitates FSK demodulation using efficient FFT algorithms, yet our experiments reveal significant demodulation time, leading to elevated power consumption [2]. Instead, the Goertzel algorithm offers faster decoding for messages with known transmitting frequencies [14]. To measure the decoding time, we run each algorithm 1000 times on the received data. On average, the CMSIS FFT takes 183400 cycles (1.91 ms), and the Goertzel implementation takes 27017 cycles (0.20 ms), which is almost a 10-fold improvement with the same decoding success rate. Therefore, a Goertzel algorithm is implemented on the microcontroller.

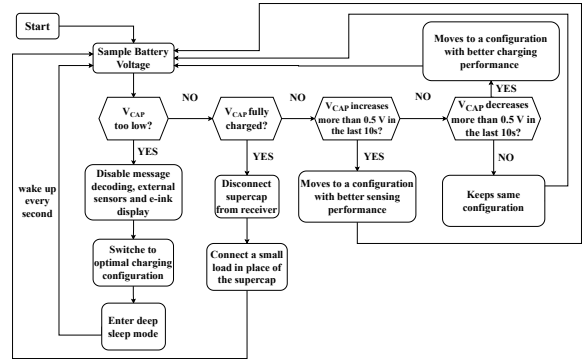


Figure 8: Receiver control loop.

5.2 Dynamic Reconfiguration

Our dynamic, reconfigurable scheme employs a feedback control system to adjust the receiver's operating points and connections. Based on the insights outlined in previous sections, the feedback control design is showcased in Figure 8. The receiver samples the supercap voltage every second, which indirectly measures the ambient light intensity. Over a 10-second period, these samples are used to estimate the charging trend in order to determine if the receiver's configuration needs to be adjusted. The changes in configuration, however, can only take effect every 16 s because that is the period determined by the MPPT algorithm. *The goal of our control scheme is to prioritize communication as much as possible while maintaining a sufficient supercap voltage.* To achieve this goal, the control scheme works as follows.

Extreme cases: The supercap is drained or fully charged. *Panic mode:* Voltage is lower than 1 V. The microcontroller stops the communication process, sets the optimal charging configuration (4s-4p), and enters a deep sleep state. The receiver continues to sample the supercap voltage, but will only exit the deep sleep mode when V_{cap} is higher than 1.2 V. *Communication-only mode:* Supercap is fully charged. The supercap is disconnected, the solar cell configuration that was in place is maintained, and a shunt resistor is connected in place of the supercap to generate a current for sensing.

Receiver is in the precharging stage. When the voltage is between 1.2 V and 1.8 V, the system loops through two configurations (2s-8p, 4s-4p) every 30 s to determine the configuration that provides the highest charging efficiency. This mode is motivated by the insights obtained in section 4, where no fixed configuration provides the best

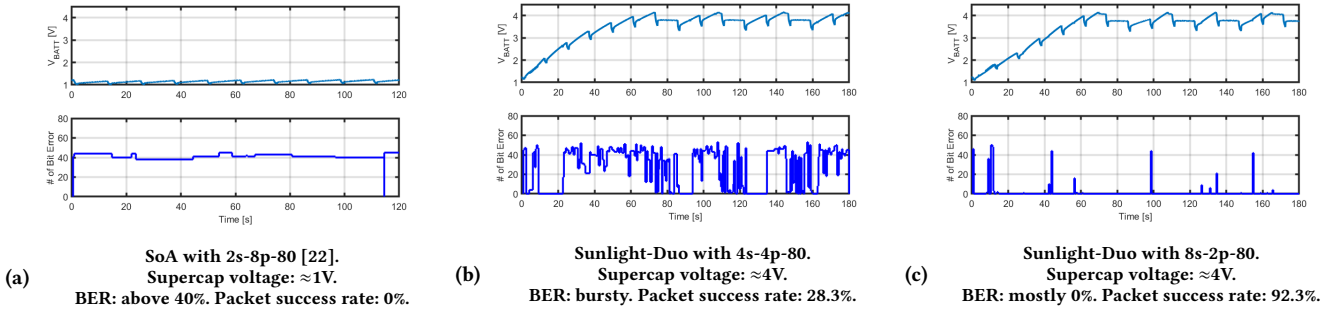


Figure 9: Comparing the SoA with Sunlight-Duo: supercap voltage and bit error rate with 50 klux interference. Under strong ambient light, the SoA guidelines cannot provide charging or communication, while Sunlight-Duo can provide both.

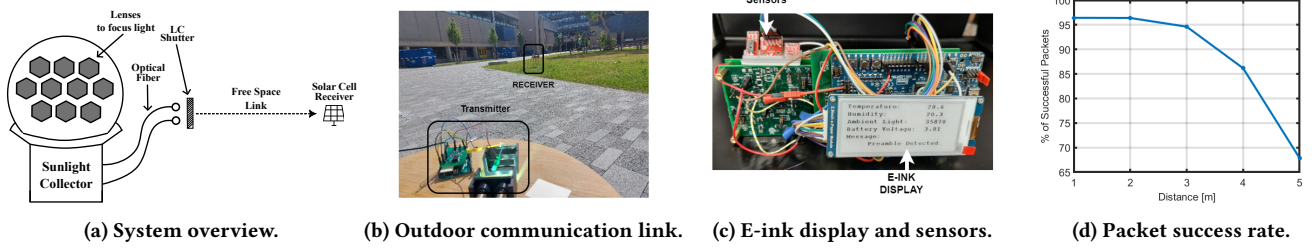


Figure 10: Outdoor experiment setup and link range

charging performance under all light intensities in the precharging state. Therefore, the receiver periodically assesses the charging performance of the two best options, parallel and mixed.

Receiver is in the charging stage. The receiver operates in one of three configurations: 8s-2p-80 (optimal charging), 8s-2p-50 (balanced performance), or 8s-2p-30 (optimal communication). If the supercap voltage is steadily increasing, the configuration is changed to prioritize communication. If the voltage remains steady, no configuration changes are made. Conversely, a declining voltage prompts a shift towards a charging-focused configuration.

6 System Evaluation

Our system evaluation addresses two critical research questions: First, can sunlight be used simultaneously as a dual-source for energy and communication? Second, is it possible to create a stable passive link where solar cells operate as both data receivers and energy harvesters?

We first undertake an indoor assessment to show that the guidelines provided by prior SoA studies do not hold in the general case. Following this, we test our prototype outdoors under different conditions. We show that Sunlight-Duo is able to communicate reliably outdoors, and further extend the system to facilitate bi-directional communication powered by sunlight. A potential application for such a system is smart farming, where sunlight coming into a greenhouse is used to collect local crop information from distributed batteryless sensors.

6.1 Comparison with the SoA

The SoA study that is the most related to ours is the one performed by Mir et al., where an LED is used as a transmitter and solar cells simultaneously power the receiver and decode data [22]. That study suggests that a series connection holds an advantage for communication, while a parallel configuration is better for charging.

Those guidelines, however, are obtained indoors in a dark room, where the signal is transmitted by a stable LED without any interference.

The SoA guidelines are valuable for a concrete scenario but do not hold universally. We use a controlled setup similar to the one presented in section 5, where we send packets, but with a key difference: To mimic a load condition representing sensors or other peripheral tasks, we use a 100Ω resistor. This resistor is connected to the supercap through an analog switch, which intermittently activates for one second every ten seconds. This setup captures an scenario where the receiver provides power for decoding and other sensing or computational tasks (intermittent load).

The transmitter (LC) is placed 1 m from the receiver. The intensity of the signal between the on and off states at the receiver is 1400 lux, strong enough to decode data with the SoA receiver. However, when we turn on the sunlight emulator, the ambient light introduces an interference of 50k lux at the receiver. We evaluate three configurations. The first configuration, suggested by the SoA [22], sets $\eta_{voc}=80\%$ and toggles between parallel (2s-8p-80) and serial (8s-2p-80) connections, contingent on whether the battery voltage (V_{batt}) is below or above 2.6V. The other two configurations are based on our analysis: mixed (4s-4p-80) and serial (8s-2p-80). Both configurations perform well in terms of charging, but the serial connection (8s-2p-80) outperforms the mixed one (4s-4p-80) in terms of communication.

Results from Figure 9 reveal that the SoA configuration fails in both, energy harvesting and packet decoding due to high BER, especially under strong light conditions where its efficiency plummets to 20% for charging and 0% for communication, as shown in Figure 9a. This leads to insufficient power for load support and a nearly random BER (50%). Conversely, our near-optimal configurations (Figure 9b and Figure 9c) successfully charge the supercapacitor

across all conditions. Specifically, the series configuration (8s-2p-80) achieves over 90% packet success rate, outperforming the mixed configuration (4s-4p-80) even amid strong ambient light. Temporary bit error spikes, due to the voltage sampling performed by the algorithm every 16 seconds, are quickly mitigated, allowing for successful packet reception. These observations underscore the importance of a thorough analysis. Our multi-step optimization shows that even with strong ambient light, the communication and harvesting capabilities of the solar cells can be preserved.

6.2 Experiment Setup in Outdoor Evaluation

In the next phase, we test our system outdoors.

Transmitter: In the outdoor experiment, we use a sunlight collector from Himawari, as shown in Figure 2c. Commercial sunlight collectors are designed to bring natural light indoors to windowless areas, but we utilize them outdoors. A sunlight collector has two functions: *collection* and *tracking*. In *collection*, the device uses lenses to gather sunlight and channel it into optical fibers, which guide the light to the desired locations. This process does not consume any power. In *tracking*, since the sun changes its location throughout the day, the lenses rotate to point toward the sun. The tracking consumes between 1 W and 2 W when the lenses are moving. We place an LC shutter in front of the optical fiber output to modulate the collected light (as seen in Figure 10b). The transmitter continuously sends "Hello World" packets at a data rate of 400 bps, unless stated otherwise.

Receiver: Thanks to the design of our low-power receiver, as described in section 5, the decoding of data is only powered by the on-board solar cell array. In addition, the receiver has three sensors: a temperature sensor (TMP102), a humidity sensor (HIH-4030), an ambient light sensor (TEMT6000); and an e-ink display DEBO EPA 2.9, which are also powered by the receiver. The e-ink display shows the measurements obtained from the sensors. An image of the receiver is shown in Figure 10. *Note that our receiver obtains light from the sun and the beam coming from the collector. Both components contribute to charging, but only the collector's beam provides the signal, the light coming directly from the sun is noise.*

6.3 Link Range and Reliability

Link range. In the first part of the experiment, the sunlight collector is placed on the ground at a fixed location, while we move the receiver to different distances. At each location, we collect the packets for a period of 30 seconds and repeat this experiment three times. At the same time, the receiver takes measurements of ambient light, temperature and humidity, and writes it to the e-ink display every 20 seconds. We also measure the average supercap voltage during the 30 second window and record it throughout the experiment. An overview of the system is provided in Figure 10a.

The packet reception rate is shown in Figure 10d. The experiment was conducted on a clear day with sunlight intensity around 60 klux. As shown, the packet success rate exceeds 85% at a distance of up to 4 m. The packet success rate does not reach 100% because communication is interrupted every 16 s when the MPPT algorithm samples the open circuit voltage. The communication distance achieved in this setup is smaller than previous passive systems using sunlight and PDs [11]. In the next subsection, we

explain how we improve the range, but first let us use Figure 11a to describe why we achieve a shorter range than the SoA.

Communication performance hinges on three factors: signal intensity (S), interference (N), and field of view (FoV). For extended range, high SNR and narrow FoV are essential. Earlier systems used mirror-like surfaces for sunlight reflection, achieving collimated patterns with less attenuation and stronger signals (large S). However, the optical fibers of sunlight collectors have a 58° FoV, which yields a broader pattern and faster signal degradation (smaller S). To achieve more collimated beams, we later show the improved range by placing lenses on the collector's beams. Another important point is that the SoA uses PDs with narrow FoVs to reduce interference (small N). Solar cells have, inherently, a wide FoV. This wide-angle cannot be reduced without affecting the energy harvesting performance. Hence, solar cell receivers face greater noise challenges (larger N).

Reliability. To test reliability, we place the receiver at a distance of 2 m from the transmitter. Daytime conditions change based on the season and specific location, in our setup daylight was obtained from 9 am to 7 pm, we recorded the link's measurements every 10 minutes for 30 seconds. During this time, the receiver powers the sensors, e-ink display and sends backscattered data. The results, in Figure 11c, show that throughout the day, a reliable link is established despite the changing environmental conditions. It can also be observed that the supercap voltage fluctuates throughout the day, as a result of the dynamic reconfiguration of the receiver. However, the receiver is able to maintain a sufficient voltage to remain as a positive-energy link.

6.4 Bi-Directional Link and Longer Range

Bi-directional link. In our star topology, the sunlight collector acts as a hub, and sensors as nodes. Until now we have only tested the downlink, to send commands from the hub to nodes. To send sensing data to the hub (uplink), we exploit the fact that the sunlight collector provides two optical fiber bundles. This setup, depicted in Figure 12a, marks the first use of sunlight for backscattering. One optical bundle is used for the downlink and the other for the uplink. The uplink employs *unmodulated* light, backscattered by a mirror at the receiver to transmit sensor data back to the transmitter, where a photosensor and processor decode the uplink data.

Extended range. In the SoA, the range is extended by adding a lens to the receiver, but this approach cannot be applied to solar cells without disrupting their energy harvesting capabilities. Instead, following basic optical principles, a lens is placed in front of the output of the sunlight collector. By incorporating a lens, we generate a narrow beam, which is roughly 120 mm when measured at 11 m, corresponding to a beam angle below 1°. In this way, we significantly reduce the signal dispersion as it travels over distance.=

Results. The results for the communication range of the downlink are shown in Figure 12b. In our test area, we could only test up to a distance of 11 m, but it can be seen that for a data rate of 400 bps, the link is strong and a longer range can be achieved thanks to the added lens. To take advantage of the higher SNR, we increase the data rate at 11 m, which is shown in Figure 12c. It can be seen that for the downlink, a packet success rate of over 90% can be achieved for a data rate of up to 1000 bps. For the uplink, a

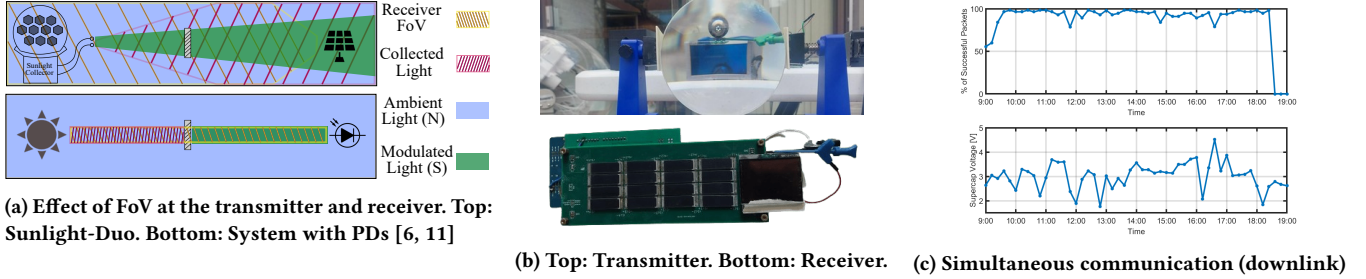


Figure 11: System Overview and experiment results.

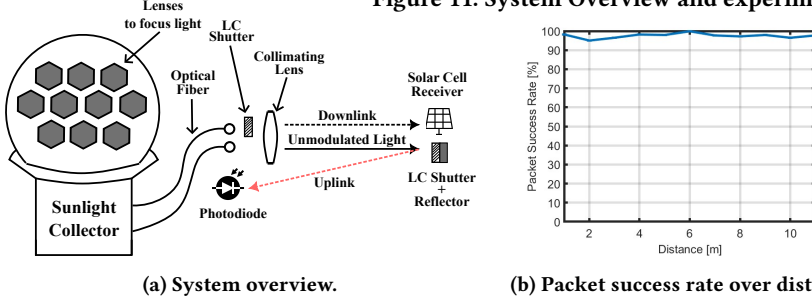


Figure 12: System and evaluation results of a bidirectional link

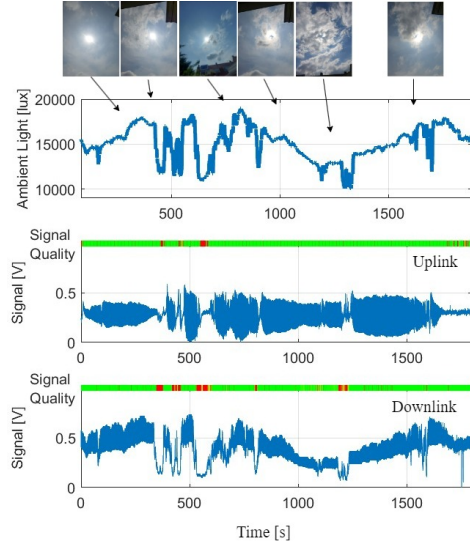


Figure 13: Link quality in a 30 minute window. Top: ambient light. Middle: uplink signal. Bottom: downlink signal.

packet success rate of over 90% can be achieved for a data rate of up to 800 bps. The uplink data rate is lower than the downlink's because the light has to travel double the distance, but they achieve a reliable bi-directional link at 11 m.

6.5 Stability of Bi-directional Link

We now assess the stability of a bi-directional communication link under fluctuating ambient light, particularly with intermittent sun blockage by clouds. We used a DFROBOT SEN0390 ambient light sensor alongside our receiver to track light intensity every second

[3]. During the evaluation, the sunlight intensity ranged between 10 klux and 18klux, which are not high values because during clear days, sunlight can provide intensities above 100 klux. In this experiment, we maintain the same setup as in the previous section, a 11 m bi-directional link, but over a 30-minute period.

The results, in Figure 13, depict the status of both uplink and downlink. The uplink showcases the AC signal post-filtering, thus excluding DC fluctuations. A color-coded system denotes the packet success rate within a one-second window: green represents a success rate over 80%, yellow between 60% and 80%, and red below 60%. For reference, we include photographs of the sky during the time. The results reveal similar stability for both uplink and downlink, although the downlink quality, affected by the double-distance travel, is slightly poorer. Total sun obstruction by clouds interrupts communication, yet during clear or moderately cloudy conditions, with the sun still visible, the link quality remains high, allowing effective communication. Over a 30-minute window, the uplink and downlink packet error rates are 90.7% and 77.8%, respectively.

6.6 Discussion

Our work provides the first link that uses sunlight for communication and power, which opens several opportunities for improvement.

Range, data rate, and line of sight. An important parameter limiting the range and data rate is the slow switching speed of inexpensive liquid crystals. As shown in Figure 2e, a full transition between the on and off states takes around 3 ms. Modulations faster than that reduce the signal-to-noise ratio because the LC cannot reach its plateau. And a reduced SNR limits either the range or data rate. Besides LCs, one alternative is to use micro-mirror devices (DMDs), which can attain several 10 kbps [30], but the system would be more complex. Another general shortcoming of light communication, compared to RF, is that without a line-of-sight (LOS),

the link degrades rapidly. In smart farming, small solar panels powering sensors are placed on bars to get LOS with the sun, but in applications without LOS the communication would be harder. To address this issue, the VLC community is investigating Intelligent Reflective Surfaces. That line of work would also benefit our system.

Comparison with alternative technologies. Sunlight-Duo leverages an abundant and sustainable resource: sunlight. However, its operation is constrained to daylight hours. While solar cells can power LEDs for active-VLC communication, this approach necessitates the use of batteries for energy storage. Moreover, converting sunlight to energy via solar cells and then converting that energy back to light through LEDs introduces inefficiencies that can be avoided by using sunlight directly, thereby eliminating the intermediary conversions. The lumen-to-watt efficiency of solar cells is 25%, and the watt-to-lumen efficiency of LEDs is 10 to 30% (95% of energy is lost). passiveVLC achieves sub- μJ per bit [31], while LEDs use 30x more energy per bit [12]. Another option is to use low-power radio systems, which are a mature technology providing longer ranges and higher data rates, but the aim of using light is to use a part of the spectrum that is free and not crowded. The best use of Sunlight-Duo is to exploit it during daylight and complement it with other technologies at night or during cloudy days. Cost and deployment are also important considerations. The sunlight collector we use costs around 4.5k USD and it is bulky because it is designed to be placed on building roofs. Considering smart farming, a cheaper alternative would be to deploy a wider array of permanent static lenses on the already transparent roofs of greenhouses, minimizing the cost and complexity of the hub. Compared to low-power RF systems, passive-VLC exploits a free and open spectrum. While RF surpasses passive-VLC in range, data rate, and energy efficiency, RF is well-established, whereas passive-VLC is emerging. Passive-VLC also eliminates double-energy conversion, offering better performance with 6 bits-per- μJ compared to lasers' 4 bits-per- μJ , without stringent regulations for eye safety and alignment. *Overall, it is important to note that our work does not aim at replacing existing technologies, but rather at presenting a complementary and novel research direction.*

7 Conclusion

This study investigates the use of sunlight as a dual-purpose medium for energy harvesting and communication. We identify and address the inherent challenges of this new type of link, especially the necessity to dynamically adjust solar cell parameters to optimize energy capture and communication effectiveness. Informed by these insights, we built a prototype that harnessed sunlight for bi-directional communication while simultaneously gathering energy. The system demonstrated a range of several meters throughout the day with a data rate of 1 kbps. To the authors' best knowledge, this is the first design that develops a complete communication and harvesting system relying only on sunlight.

Acknowledgments

The authors would like to thank the reviewers for their feedback. This work has been funded by the European Union's H2020 programme under the Marie Skłodowska Curie grant agreement ENLIGHTEM No. 814215, and by the Dutch Research Council (NWO) with a TOP-Grant with project number 612.001.854.

References

- [1] Apollo3 blue plus. https://wiki.dfrobot.com/Ambient_Light_Sensor_0_200klx_SKU_SEN0390#target_0.
- [2] Cmsis dsp software library. <https://www.keil.com/pack/doc/CMSIS/DSP/html/index.html>. Accessed: 2022-09-01.
- [3] Dfrobot sen0390. <https://ambiq.com/apollo3-blue-plus>.
- [4] Global progress in photovoltaic technologies and the scenario of development of solar panel plant and module performance estimation application in nigeria. *Renewable and Sustainable Energy Rev.*, 2015.
- [5] D. Bharadia et al. Backfi: High throughput wifi backscatter. 2015.
- [6] R. Bloom et al. Luxlink: Creating a wireless link from ambient light. In *ACM Sensys*, 2019.
- [7] Cisco. Cisco annual internet report (2018–2023) white paper. 2020.
- [8] S. Das et al. Towards energy neutral wireless communications: Photovoltaic cells to connect remote areas. *Energies*, 2019.
- [9] S. Das et al. Effect of sunlight on photovoltaics as optical wireless communication receivers. *Journal of Lightwave Technology*, 2021.
- [10] P. D. Diamantoulakis et al. Simultaneous lightwave information and power transfer. *IEEE Transactions on Green Communications and Networking*, 2018.
- [11] S. K. Ghiasi et al. A principled design for passive light communication. ACM Mobicom, 2021.
- [12] B. G. Guzman et al. Prototyping visible light communication for the internet of things using openvlc. *Comm. Mag.*, 61(5):122–128, may 2023.
- [13] H. Haas et al. What is lifi? *Journal of Lightwave Technology*, 2016.
- [14] D. Jones. Goertzel's algorithm. *This recently updated page provides a concise mathematical treatment of the Goertzel Algorithm in its general form*, 2006.
- [15] S. Kim et al. Simultaneous reception of visible light communication and optical energy using a solar cell receiver. In *2013 International Conference on ICT Convergence (ICTC)*.
- [16] J. Li et al. Retro-VLC: Enabling battery-free duplex visible light communication for mobile and iot applications. ACM HotMobile, 2015.
- [17] Y. Li et al. Self-powered gesture recognition with ambient light. ACM UIST, 2018.
- [18] V. Liu et al. Ambient backscatter: Wireless communication out of thin air. *SIGCOMM Comput. Commun. Rev.*, 2013.
- [19] N. Lorriére et al. Photovoltaic solar cells for outdoor lifi communications. *Journal of Lightwave Technology*, 2020.
- [20] D. Mir et al. Solargest: Ubiquitous and battery-free gesture recognition using solar cells. ACM MobiCom, 2019.
- [21] L. E. M. Matheus et al. Visible light communication: Concepts, applications and challenges. *IEEE Comm. Surveys & Tutorials*, 2019.
- [22] M. S. Mir et al. Passivelifi: Rethinking lifi for low-power and long range rf backscatter. ACM MobiCom, 2021.
- [23] G. Pan et al. Simultaneous lightwave information and power transfer: Policies, techniques, and future directions. *IEEE Access*, 2019.
- [24] N. V. Huynh et al. Ambient backscatter communications: A contemporary survey. *IEEE Communications Surveys Tutorials*, 2018.
- [25] P. Wang et al. Renovating road signs for infrastructure-to-vehicle networking: A visible light backscatter communication and networking approach. ACM MobiCom, 2020.
- [26] Q. Wang et al. Passive visible light networks: Taxonomy and opportunities. In *Proceedings of the Workshop on Light Up the IoT*, 2020.
- [27] Z. Wang et al. Towards self-powered solar panel receiver for optical wireless communication. In *IEEE ICC*, 2014.
- [28] Z. Wang et al. On the design of a solar-panel receiver for optical wireless communications with simultaneous energy harvesting. *IEEE Journal on Selected Areas in Communications*, 2015.
- [29] Y. Wu et al. Turboboosting visible light backscatter communication. ACM SIGCOMM, 2020.
- [30] T. Xu et al. Exploiting digital Micro-Mirror devices for ambient light communication. In *USENIX NSDI*, 2022.
- [31] X. Xu et al. Enabling practical visible light backscatter communication for battery-free iot applications. ACM MobiCom, 2017.